THE JOURNAL OF PHYSICAL CHEMISTRY LETTERS
A JOURNAL OF THE AMERICAN CHEMICAL SOCIETY

Open Access
This article is licensed under CC-BY 4.0

pubs.acs.org/JPCL
Letter

Mapping the Energy Transfer Network in the Diatom *Cyclotella meneghiniana* by Picosecond Time-Resolved Fluorescence Spectroscopy down to Cryogenic Temperatures

Lena Golubewa, Yaraslau Padrez, Marius Franckevičius, Patricija Zemaityte, Simona Streckaitė, Jevgenij Chmeliov, Leonas Valkunas, Bruno Robert, Claudia Büchel, and Andrius Gelzinis*

Cite This: *J. Phys. Chem. Lett.* 2026, 17, 10191−10198

Read Online

ACCESS | Metrics & More | Article Recommendations | Supporting Information

ABSTRACT: Diatoms are unicellular photosynthetic microalgae that contribute nearly a quarter of the global primary production. Knowledge of the mechanisms, networks, and time scales of the excitation transfer is crucial for a deeper understanding of their photosynthetic machinery. Unfortunately, the short excited-state lifetime of photosystem I at room temperature and research focus on isolated structures have limited the development of a complete excitation transfer scheme in intact cells. Here, we address this gap through picosecond time-resolved fluorescence measurements on intact *Cyclotella meneghiniana* cells obtained from 16 to 130 K and room temperature. Analysis of the data in terms of evolution-associated spectra reveals a complex interplay of excitation transfer, population of fluorescing trapping states, and excitation quenching at the whole-cell level. We show rapid depopulation of all antenna complexes, on the order of 30 ps even at 16 K, indicating a more efficient energy-transfer network in diatoms than in higher plants.

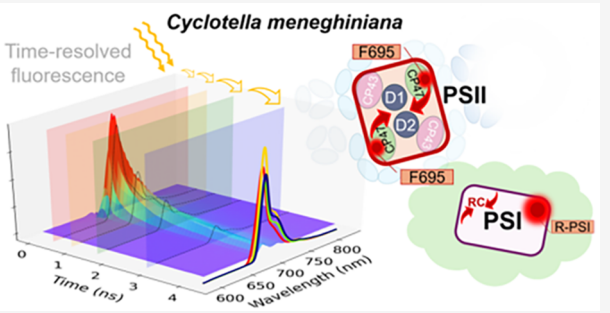

Diatoms are a major group of marine algae that account for almost a quarter of the global primary production.[1−3] They also contribute heavily to major biochemical cycles of carbon, silicon, nitrogen, and phosphorus. To survive under widely fluctuating light conditions present in their underwater habitat, diatoms have developed a very efficient photosynthetic machinery.[4,5] They contain the same photosystems I and II (PSI and PSII) also found in green algae and higher plants. On the other hand, the light-harvesting antenna of diatoms is composed of fucoxanthin−chlorophyll protein (FCP) complexes. They are specifically adapted to harvest the blue−green light, as they contain a large number of carotenoid [mainly fucoxanthin (Fx)] molecules as well as chlorophyll *c* (Chl *c*) instead of Chl *b*.[6]

Recently, numerous studies have revealed the atomic structures of PS−FCP supercomplexes as well as those of isolated FCPs from various diatoms.[7−14] These results form a solid basis for interpreting the time-resolved spectroscopic data obtained on isolated (super)complexes from these organisms.[15−28] Such studies, while providing insights into the energy transfer in the constituents of the photosynthetic machinery, cannot reveal a complete picture of the excitation dynamics in the whole cells. Unfortunately, time-resolved spectroscopic investigations on the level of the whole cell are much rarer.[29−34] In this work, we will attempt to fill this void.

Even though photosynthesis takes place at room temperature (RT), in such conditions, spectroscopic investigations of the whole photosynthetic apparatus are hindered by overlapping bands and the extremely short excited-state lifetime of PSI.[35] Therefore, temperature-dependent studies, similar to what was previously done on aggregates of the major light-harvesting complexes of PSII (LHCII) from higher plants,[36] aggregates of FCP complexes,[26] as well as chloroplasts from wild-type and mutant plants,[37] could reveal excitation transfer pathways and time scales in intact cells.

Here, we present streak-camera time-resolved fluorescence (FL) measurements on *Cyclotella meneghiniana* cells grown under low-light (LL) conditions at a broad temperature range of 16−130 K and RT (see the Experimental Methods). It must be stressed that our recent investigation on diatom cells has revealed that application of glycerol, a usual cryoprotectant, damages cells and significantly affects the photosynthetic apparatus.[38] Thus, in this study, cells were frozen in medium without glycerol. In Figure 1, we present the time- and wavelength-resolved FL measurements on *C. meneghiniana* at 16 K, with the excitation wavelength being 515 nm, thus

Received: June 30, 2026
Revised: August 12, 2026
Accepted: August 14, 2026
Published: August 19, 2026



ACS Publications
© 2026 The Authors. Published by American Chemical Society

https://doi.org/10.1021/acs.jpclett.6c02173
J. Phys. Chem. Lett. 2026, 17, 10191−10198

Downloaded from pubs.acs.org/jpclcd/article-pdf/17/35/10191/6688584/acs.jpclett.6c02173.pdf by VILNIUS UNIV user on 12 November 2026

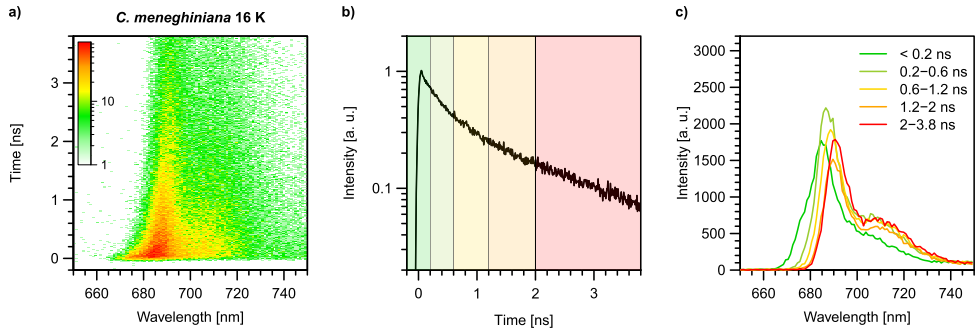

Figure 1. Streak-camera FL data of *C. meneghiniana* cells at 16 K upon excitation at 515 nm: (a) two-dimensional FL map, (b) normalized FL kinetics, integrated over the measured spectral region, and (c) integrated FL spectra at different time intervals that correspond to the shaded regions in panel b.

targeting mainly carotenoids. The main FL band, visible in the two-dimensional FL map in Figure 1a, is at 690 nm. There is also a weaker band at 700−720 nm as well as a short-lived band at 675−680 nm. The wavelength-integrated kinetics, presented in Figure 1b, demonstrate that the total FL signal decreases by an order of magnitude in about 3 ns. Nonetheless, this integrated characteristic does not reveal the full picture of excitation decay, since the spectra corresponding to different time intervals exhibit a complex pattern, with a red shift of the main FL band from ∼685 nm at early times to ∼690 nm at later times as well as an increase of the intensity of the red band at 700−720 nm (see Figure 1c). Data for other temperatures are presented in Figures S1 and S2 of the Supporting Information.

Temperature dependence of the FL data is shown in Figure 2. At room temperature, fluorescence is mainly due to PSII and FCPs. The time-integrated spectrum at room temperature (Figure 2a) is dominated by the main band fluorescing at ∼681 nm, which corresponds to the Chl *a* Q_y band of PSII, with a weak vibrational shoulder also visible. As the temperature gets lower, the main band exhibits a red shift, reaching ∼690 nm at 16 K. In addition, the intensity of the broad red band at 700−720 nm increases, signifying a larger contribution from PSI. There is some scatter in the temperature dependence, as can be expected for complex biological samples, but the trends are clear. Considering next the wavelength-integrated kinetics (Figure 2b), the slowest decay is at 16 K, and the decay becomes faster as the temperature increases up to 130 K, albeit with some scatter. Interestingly, the RT kinetics exhibit a slower decay than some of the low-temperature kinetics, though the trend suggests that it lacks the longest lifetime component that is apparent at lower temperatures.

To extract information present in the obtained temperature-dependent FL data sets, we applied evolution-associated spectra (EAS) analysis.[39] It is a type of global analysis that assumes sequentially connected compartments, with only the first one being excited at the initial time. The population from the first compartment decays to the next one with time scale τ_1, and this process continues up to the *N*th compartment, which decays to the ground state with time scale τ_N. Even though the component spectra obtained in such a way do not represent single emitting species, they represent characteristic spectra of the fluorescing states at particular times. Thus, the parallel dynamics occurring in PSII and PSI supersystems are described by an effective model, with each of the EAS containing signatures of both. Due to the absence of PSII and PSI reference streak camera data from *C. meneghiniana* and the very high signal-to-noise ratio required for such analysis, which is difficult to obtain for cells, a full kinetic scheme was not employed.

The spectral components corresponding to *C. meneghiniana* FL data at different temperatures are shown in Figure 3 along with the decay time scales. The RT data were adequately described by three components, while all low-temperature spectra were described by four components. The dependence of each spectral component on the temperature (except for RT) is presented in Figure S3. For the low-temperature data, the spectral shapes and time scales of each component change in a consistent manner upon changes in the temperature, signifying that EAS constitute a reasonable data representation.

Let us consider the RT data first. All the components are very similar to each other and, thus, to the integrated spectrum, with the maximum of the main band at ∼681 nm. Interestingly, it is blue-shifted by ∼2 nm to what can be expected from the FL of the PSII core.[40] Note that the isolated PSII antenna complexes from *C. meneghiniana* fluoresce at shorter wavelengths, 678 nm for the trimeric FCPa and 674 nm for the non-americ FCPb, at RT.[26] The first component is quite noisy, but it suggests a somewhat larger amplitude in the 700−740 nm spectral region, which would correspond to the very rapidly decaying contribution of the PSI fluorescence. The second and third time scales are similar to the first two time scales obtained in ref 30 for cells excited at 535 nm.

Next we turn to the low-temperature data. The initial spectra are reflected by EAS1. This is the most blue-shifted spectral component, with its maximum at 677 nm at 16 K (see Figure 3 and Figure S3). At higher temperatures, EAS1 red shifts and broadens. It is natural to assign this spectral component to the FCP antenna associated with PSII. FCPs fluoresce at wavelengths around 680 nm at lower temperatures.[26] Our excitation wavelength of 515 nm excites mostly carotenoids,[41] and because there are significantly more carotenoids in the antenna complexes rather than in the PSII core,[14] it is the antenna that should be preferentially excited at the initial times. This component decays with a 20−40 ps time scale. It might be tempting to relate this time scale to intracomplex transfer from higher energy Chl *a* to lower energy Chl *a* in the FCP antenna. Such explanation could be discarded, however, since in isolated FCPs, no significant peak shift at early times is observed and the fluorescence maxima (see ref 26 and Figure S4) are at shorter wavelengths than that of EAS2. Therefore, our results demonstrate very fast energy transfer from the FCP antenna to the PSII core even at 16 K. Note that the time

https://doi.org/10.1021/acs.jpclett.6c02173
J. Phys. Chem. Lett. 2026, 17, 10191−10198

Downloaded from pubs.acs.org/jpclcd/article-pdf/17/35/10191/6688584/acs.jpclett.6c02173.pdf by VILNIUS UNIV user on 12 November 2026

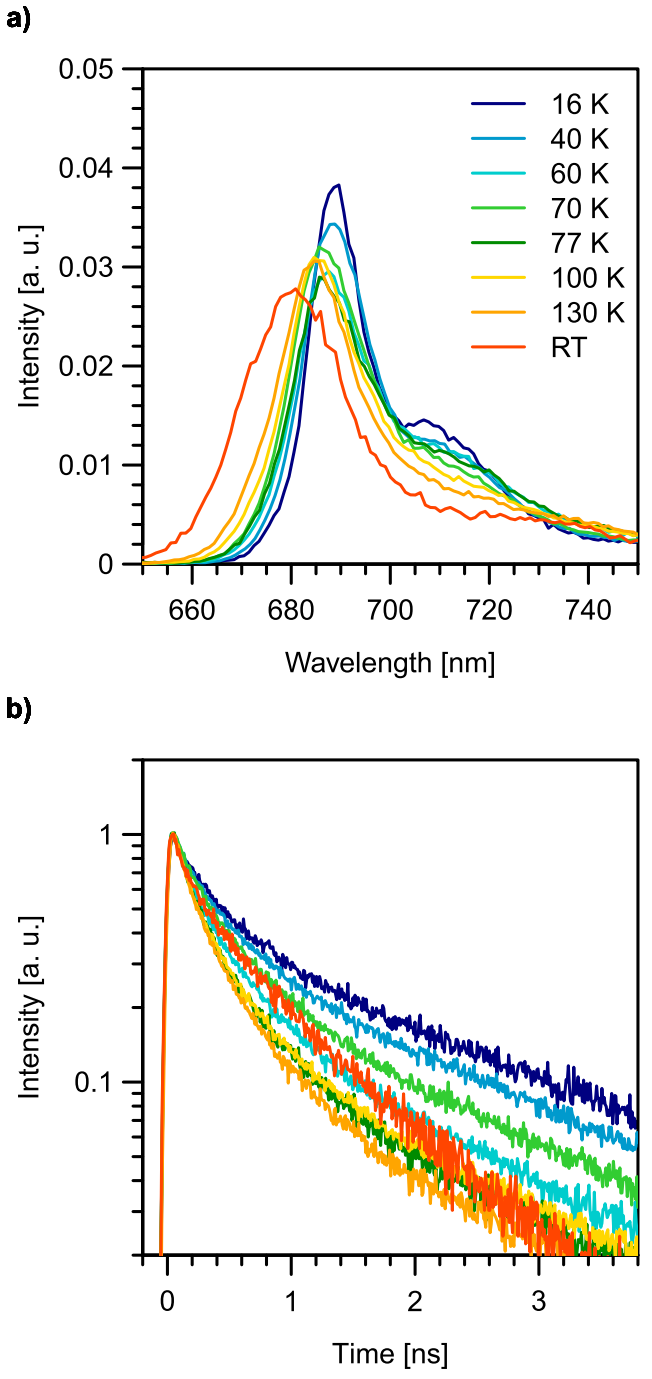

Figure 2. Integrated FL data of *C. meneghiniana* cells at different temperatures: (a) time-integrated FL spectra normalized to unit area and (b) normalized wavelength-integrated FL kinetics. The legend in panel a also applies for panel b.

scales obtained from the fitting procedure in the EAS analysis are somewhat shorter than our time resolution of ∼60 ps; thus, they have to be interpreted with some caution. Recently, extremely fast (<5 ps) energy transfer from closely associated antenna complexes to the core was observed in the PSII−FCPII supercomplexes from another diatom *Thalassiosira pseudonana* down to 77 K by two-dimensional electronic spectroscopy.[25] Here, we demonstrate very fast transfer on the whole cell level down to 16 K.

It must be noted that the FL spectra of the isolated FCPa/b antenna complexes exhibit a blue shift with an increasing temperature,[26] while EAS1 shows an opposite trend (see Figure 3 and Figure S3). Therefore, additional fluorescent states should contribute to this component. Since our excitation conditions preferentially excite carotenoids, FCPs associated with PSI (FCPI) should also be excited at the initial time, more strongly than the PSI core. Having this in mind, we can conclude that EAS1 also contains signatures of energy transfer from the FCPIs to the PSI core. A similar fast transfer time scale, on the order of 20 ps, was demonstrated for the PSI−FCPI supercomplex from *T. pseudonana* down to 77 K.[27]

Let us turn our attention to EAS2. The main peak position shifts from ∼685 nm at low temperatures to ∼682 nm at 130 K (see Figure 3 and Figure S3). It is known that CP43 should fluoresce at 683−684 nm,[42] and the PSII reaction center (RC) should fluoresce at 682−684 nm.[43] On the other hand, CP47 fluoresces at 690−695 nm at very low temperatures due to the presence of a low-energy Chl molecule.[44,45] We can thus conclude that EAS2 reflects FL from the PSII core, with excitation not yet in the equilibrium state. The decay time scales are ∼130 ps at low temperatures to 45 ps at 130 K, and they correspond to a step in the equilibration process. Based on the time-resolved FL study on PSI−FCPI from another diatom *Chaetoceros gracilis* at 77 K,[24] FL from PSI should also contribute to EAS2 at ∼700 nm.

Considering next EAS3, its spectral maxima shifts from ∼687 nm at 16 K to ∼685 nm at 130 K (see Figure 3 and Figure S3). This leads to the conclusion that a considerable portion of the FL should originate in the trap Chl of the CP47 complex, yet the equilibration in the PSII core is not complete. At lower temperatures, EAS3 also shows explicit signatures of an additional fluorescing state at ∼710 nm. It should correspond to red-emitting states in the PSI core. The fluorescence from PSI core complexes from *T. pseudonana* exhibits a broad band at 700−720 nm.[27] Similar red-emitting states are expected for PSI from *C. meneghiniana*. Even though currently there is no fluorescence data from the PSI core complexes from *C. meneghiniana*, isolated PSI antenna-containing supercomplexes exhibit a red-emitting fluorescence band at ∼716 nm at 77 K.[46] Excitation thus begins to reach the red-emitting states in the PSI complexes within the time scale of EAS2, ≲130 ps. On the other hand, the time scale of EAS3 corresponds to the characteristic time for excitation to reach the equilibrated state (EAS4 in our model). Thus, the equilibration time scale ranges from ∼500 ps at 16 K to ∼300 ps at 130 K in *C. meneghiniana* cells.

Finally, let us discuss EAS4. It should correspond to the FL from the equilibrated states in both the PSII and PSI supercomplexes. The maxima of the main band shifts from ∼692 nm at low temperatures to ∼685 nm at 130 K (see Figure 3 and Figure S3). Thus, at the lowest temperature, FL should originate in the trap Chl of the CP47 complex (F695 state[40]), while at higher temperatures, at least some excitation probably resides on other low-energy states of the PSII core. In EAS4, the ∼710 nm FL band becomes pronounced at lower temperatures. This should reflect the excitation from the entire PSI supercomplex being transferred to the red-emitting states in the PSI core, which are deeper excitation traps than the P700 state in the RC. The time scale of EAS4 describes the decay of the excitation to the ground state. It is ∼2.5 ns at very low temperatures and speeds up significantly to 1.3 ns at 130 K. Quenching in the PSII supercomplexes likely corresponds to energy transfer to the PSII RC. At all low temperatures considered in this work, the RCs can become closed due to

Downloaded from pubs.acs.org/jpclcd/article-pdf/17/35/10191/6688584/acs.jpclett.6c02173.pdf by VILNIUS UNIV user on 12 November 2026

https://doi.org/10.1021/acs.jpclett.6c02173
J. Phys. Chem. Lett. 2026, 17, 10191−10198

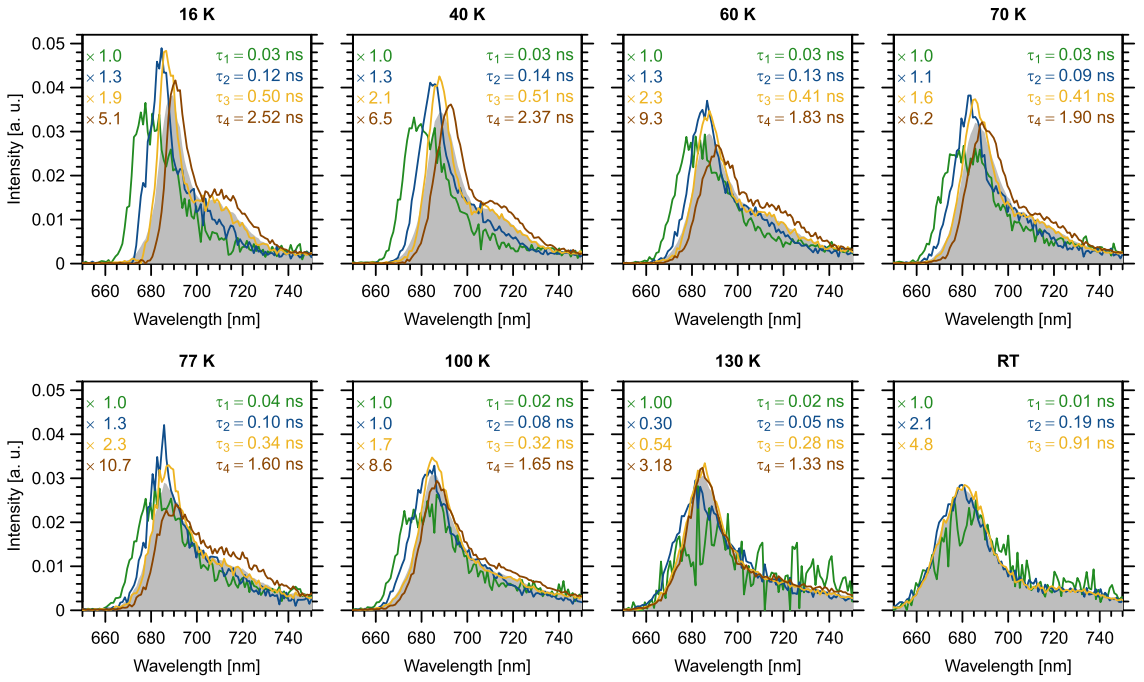

Figure 3. EAS analysis of *C. meneghiniana* FL data. Spectral components are normalized to unit area, which results in relative multiplicative factors listed on the left of each panel. Time scales of the corresponding EAS components are listed on the right of each panel. Shaded gray areas represent the time-integrated spectra normalized to unit area.

excitations,[47] but even a closed RC is an efficient quencher.[48] The time scale of EAS4 should be related to the time excitations needed to escape the trapping states and reach the quenching site in both PSs. It is also interesting to note that the majority of the observed fluorescence signal in cells is not from the equilibrated state represented by EAS4 but rather the intermediate state EAS3. This can be seen from Figure 3 by comparing the areas of the component spectra to that of the integrated spectra. Similar situations can be encountered in isolated photosynthetic complexes as well. For example, in PSII core complexes, excitation can only partially reach the trapping state F695 before it relaxes to the ground state. Interestingly, the time scales and shapes of EAS4 in our data are quite similar to the longest component decay-associated spectra for PSII cores.[49]

The observed complex dynamics in the system is difficult to describe with a single lifetime. Thus, we have estimated the lifetime as a function of the wavelength (see the Experimental Methods), which is illustrated in Figure 4. At 16 K, the mean lifetimes are ∼1.5 ns at 690 nm and ∼1.8 ns at 730 nm. The states at ∼675 nm have a ∼100 ps lifetime, which is much shorter than that at 690 nm and is related to the fast energy transfer from FCPs to PS cores. Upon an increase of the temperature, the lifetimes of the main FL bands decrease, even though the temperature dependence exhibits some scatter. At 77 K, the mean lifetimes are ∼0.5 ns from 690 to 730 nm. They become even faster at 130 K. On the other hand, at room temperature, the mean lifetimes slightly increase.

The fact that the mean lifetimes are shorter at 130 K than at RT could be explained as follows. The differences between the excitation energies in the antenna complexes and those in the PSII core complexes are not very big. At high temperatures, the excitation can rapidly transfer from the antenna to the core but can also return to the antenna. At slightly lower temperatures,

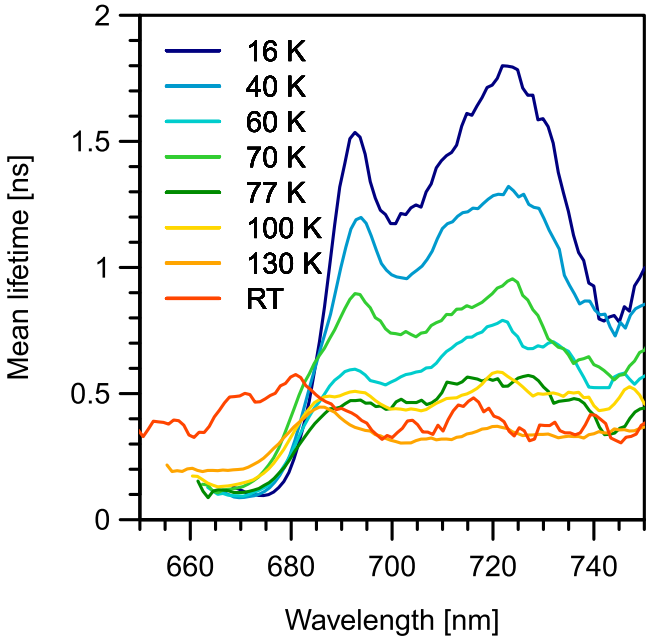

Figure 4. Estimated dependence of the mean excitation lifetime on the wavelength for *C. meneghiniana* cells at different temperatures.

the energy migration thus could be slightly more directional toward the core and, correspondingly, toward the quenching trap. At even lower temperatures, this effect is countered by the general slow down of energy transfer as well as possibilities for excitation to get stuck in the fluorescing traps in CP47 and CP43.

Our results from the low-temperature time-resolved FL experiments are summarized in the schematic illustration of the electronic excitation dynamics in *C. meneghiniana* cells,

Downloaded from pubs.acs.org/jpclcd/article-pdf/17/35/10191/6688584/acs.jpclett.6c02173.pdf by VILNIUS UNIV user on 12 November 2026

https://doi.org/10.1021/acs.jpclett.6c02173
J. Phys. Chem. Lett. 2026, 17, 10191−10198

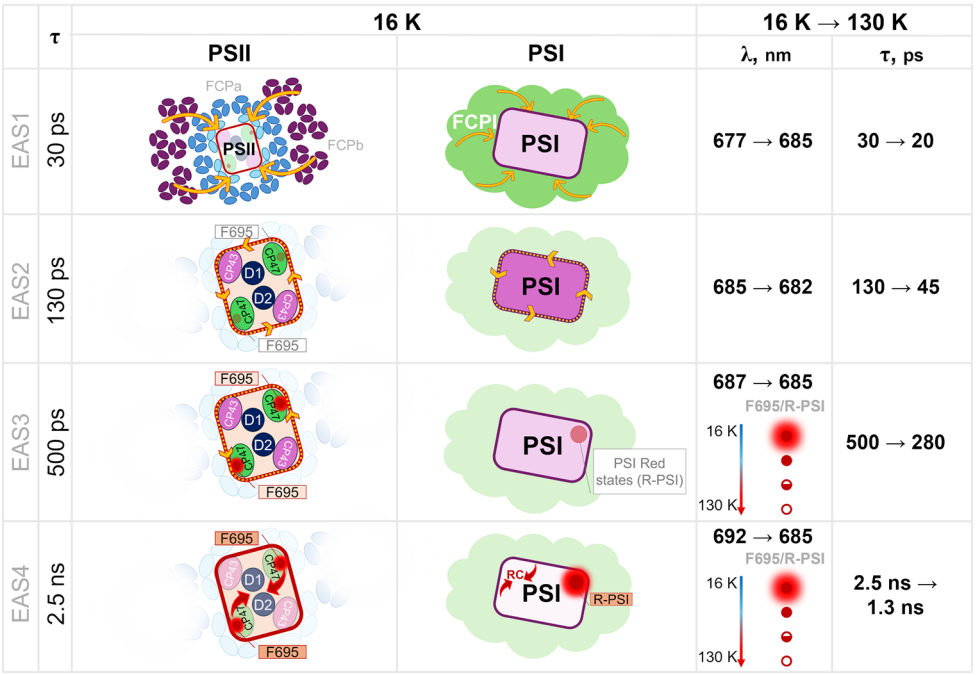

Figure 5. Schematic illustration of the electronic excitation dynamics in *C. meneghiniana* cells, as observed from the streak-camera FL measurements. Each row is associated with a different EAS component. The left side of the figure corresponds to 16 K data. Drawings indicate the molecular compartments responsible for the observed spectral shapes and time scales for the PSII and PSI complexes with the FCPs associated with them. The right side of the figure illustrates the main changes upon increasing temperature. See the text for details.

presented in Figure 5. Rows illustrate the dynamics corresponding to each EAS component. For 16 K, the scheme illustrates the major processes occurring in both the PSII and PSI complexes. Let us consider the former first. After the excitation of the system, energy is transferred from the FCP antenna to the PSII core on a 30 ps time scale. The next step is an intermediate one, during which the population begins to equilibrate within the PSII core on a 130 ps time scale. The system then reaches an equilibrated state with a 500 ps time scale, which corresponds to the majority of the population being in the F695 trapping state of the CP47 complex. The excitation is quenched with a 2.5 ns time scale, during which excitation escapes the F695 state and reaches the quenching state in the PSII RC, which is in the D1/D2 proteins. In the PSI supercomplex, the initial step after excitation corresponds to energy transfer to the PSI core. During the next step, excitation equilibrates in the core. Then, excitation begins to reach red-emitting states in the PSI core, which act as fluorescing excitation traps. Finally, most of the excitation reaches the trapping states, and the overall decay is due to detrapping and transfer to the RC, where quenching occurs. Upon an increase of the temperature, the processes become faster, with time scales of each of the EAS components decreasing. The initial spectra, corresponding to EAS1, exhibit a red shift, while the spectra of the later components become blue-shifted. The latter effect is related to a smaller population of the F695 state with an increasing temperature. For the PSI supercomplexes, the temperature increase similarly results in a smaller population of red-emitting states in the PSI core.

It must be stressed that our experiments were performed on *C. meneghiniana* cells grown under LL conditions. Different light conditions could result in some adjustments to the energy transfer picture described above. FCPs from cells grown under high light (HL) differ in polypeptide composition and have slightly different pigment stoichiometries.[50] In addition, FL from HL cells exhibits faster quenching and a weaker PSI signal.[30]

In summary, our time-resolved FL measurements at RT and on intact-frozen *C. meneghiniana* cells at low temperatures reveal a complex interplay of excitation transfer, population of fluorescing trapping states, and excitation quenching. At low temperatures, we observe equilibration of excitation in the photosynthetic machinery on time scales ranging from 500 ps at 16 K to 280 ps at 130 K. Importantly, our results demonstrate extremely fast, on the order of 30 ps, depopulation of FCP antenna complexes even at the lowest temperatures. It is important to note that this includes all of the antenna complexes and not only the ones closest to the cores. These results imply a very efficient energy-transfer network in *C. meneghiniana* cells. Interestingly, it appears to be more efficient than the one in higher plants, for which recent work suggested a 50 ps transfer time scale from neighboring major and minor antenna complexes to the PSII core.[51] Such an efficient energy transfer network clearly shows highly optimized structural organization of the PS−FCP supercomplexes.

Experimental Methods

The centric diatom *C. meneghiniana* (Culture Collection Göttingen, strain 1020-1a) was grown in batch cultures at 15 °C under low light (20 μmol of photons m^{-2} s^{-1}) with 16:8 h light/dark cycles and constant shaking in silica-enriched Provasoli's artificial seawater (ASP)[52] medium. Cells for measurements were harvested during the logarithmic growth phase, and their concentration was adjusted so that the final optical density measured at the Chl *a* Q_y band using a JASCO V-670 spectrometer (Jasco, U.S.A.) was 0.05−0.10. For streak-camera measurements, the cells were dark-adapted for 10−15 min and measured in ASP without added glycerol to preserve

https://doi.org/10.1021/acs.jpclett.6c02173
J. Phys. Chem. Lett. 2026, 17, 10191−10198

Downloaded from pubs.acs.org/jpclcd/article-pdf/17/35/10191/6688584/acs.jpclett.6c02173.pdf by VILNIUS UNIV user on 12 November 2026

cell viability prior to freezing. Measurements were performed using a circular fused silica cell with a 0.5 mm optical path, hermetically sealed with a thin strip of paraffin film. Time-resolved fluorescence spectroscopy measurements were performed using a streak camera (Hamamatsu C5680) with a M5677 (single-sweep) module coupled to a spectrometer and a femtosecond Yb:KGW oscillator (Pharos, Light Conversion, Ltd.) with a frequency doubler (HIRO, Light Conversion, Ltd.) producing 515 nm sub-100 fs pulses as the excitation source. The repetition rate was reduced to 20 kHz in single-sweep mode. A 4 ns time window was used. The full width at half maximum of the instrument response function was approximately 60 ps. Measurements were performed in a closed-cycle helium cryostat (Janis Research Company, LLC) at temperatures ranging from 15 K to RT. First, measurements at RT were performed to measure intact cells. Next, the fused silica cell with *C. meneghiniana* suspension was cooled to 15 K and then subsequently heated and measured at specific temperatures (16, 40, 60, 70, 77, 100, and 130 K). According to our previous research,[38] cells at higher temperatures than 130 K could already be affected by the start of the thawing process. For measurements at all temperatures, no significant intensity fluctuations nor changes in the spectral shapes or kinetics were observed during the course of measurements. Since only four temperatures could be measured per day, the complete set of temperature measurements was accumulated within 3−4 days. To account for possible variability between cells measured on different days, several specific temperatures were repeated each day to enable data set comparison and estimation of cell-culture-related variance. Three sets of similar measurements were performed.

Due to the scattering nature of the sample, the peak wavelengths were shifted in the measurements. As a correction, the wavelength axis for each measurement was shifted so that the integrated spectrum matched the one obtained from measurements using time-correlated single photon counting spectrofluorometer Edinburgh Instruments FLS920. To improve the signal-to-noise ratio, spectra measured at the same temperature (at 40, 77, 100, and 130 K) within the same set were added. Jitter correction was applied for all measured data. The background was removed from all the spectra. EAS were obtained following ref 39 by custom written R scripts.[53] Mean lifetime dependence on the wavelength was estimated from decay-associated spectra (DAS) analysis[39] as $\tau_{avg}(\lambda) = \sum_i' A_i(\lambda)\tau_i / \sum_i' A_i(\lambda)$. Here, A_i denotes the amplitude of each DAS, and the prime over the sum means that only components for which $A_i(\lambda) > 0$ were included in the sum. Three-component DAS analysis was used, because using four components for 130 K and RT data resulted in the presence of two components of similar magnitude but opposite sign.

■ ASSOCIATED CONTENT

Supporting Information

The Supporting Information is available free of charge at https://pubs.acs.org/doi/10.1021/acs.jpclett.6c02173.

Streak-camera FL data of *C. meneghiniana* cells corresponding to 16, 40, 60, and 70 K (Figure S1) and 77, 100, and 130 K and RT (Figure S2), temperature dependence (except for RT) of the spectra of each EAS component for the *C. meneghiniana* FL data (Figure S3), and two-component EAS analysis for FCPb complexes (Figure S4) (PDF)

■ AUTHOR INFORMATION

Corresponding Author

Andrius Gelzinis − *Department of Molecular Compound Physics, Center for Physical Sciences and Technology, 10257 Vilnius, Lithuania; Institute of Chemical Physics, Faculty of Physics, Vilnius University, 10222 Vilnius, Lithuania;* orcid.org/0000-0001-5902-0506; Email: andrius.gelzinis@ftmc.lt

Authors

Lena Golubewa − *Institute of Chemical Physics, Faculty of Physics, Vilnius University, 10222 Vilnius, Lithuania; Department of Molecular Compound Physics, Center for Physical Sciences and Technology, 10257 Vilnius, Lithuania;* orcid.org/0000-0003-2125-6366

Yaraslau Padrez − *Department of Molecular Compound Physics, Center for Physical Sciences and Technology, 10257 Vilnius, Lithuania; Neuroscience Research Center, College of Medicine, Jiaxing University, Jiaxing, Zhejiang 314001, China;* orcid.org/0000-0003-0852-6579

Marius Franckevičius − *Department of Molecular Compound Physics, Center for Physical Sciences and Technology, 10257 Vilnius, Lithuania;* orcid.org/0000-0001-8020-7201

Patricija Zemaityte − *Department of Molecular Compound Physics, Center for Physical Sciences and Technology, 10257 Vilnius, Lithuania; Life Science Center, Vilnius University, 10257 Vilnius, Lithuania*

Simona Streckaitė − *Department of Molecular Compound Physics, Center for Physical Sciences and Technology, 10257 Vilnius, Lithuania;* orcid.org/0000-0003-0541-5806

Jevgenij Chmeliov − *Department of Molecular Compound Physics, Center for Physical Sciences and Technology, 10257 Vilnius, Lithuania; Institute of Chemical Physics, Faculty of Physics, Vilnius University, 10222 Vilnius, Lithuania;* orcid.org/0000-0002-7591-1373

Leonas Valkunas − *Department of Molecular Compound Physics, Center for Physical Sciences and Technology, 10257 Vilnius, Lithuania;* orcid.org/0000-0002-1356-8477

Bruno Robert − *Université Paris-Saclay, CEA, CNRS, Institute for Integrative Biology of the Cell (I2BC), 91198 Gif-sur-Yvette, France;* orcid.org/0000-0001-5999-4538

Claudia Büchel − *Institute of Molecular Biosciences, Department of Biosciences, Goethe University Frankfurt, 60438 Frankfurt, Germany;* orcid.org/0000-0001-6640-7610

Complete contact information is available at: https://pubs.acs.org/10.1021/acs.jpclett.6c02173

Notes

The authors declare no competing financial interest.

■ ACKNOWLEDGMENTS

This work was supported by the Research Council of Lithuania (LMTLT, Project S-PD-24-158).

■ REFERENCES

(1) Nelson, D. M.; Tréguer, P.; Brzezinski, M. A.; Leynaert, A.; Quéguiner, B. Production and dissolution of biogenic silica in the ocean: Revised global estimates, comparison with regional data and

Downloaded from pubs.acs.org/jpclcd/article-pdf/17/35/10191/6688584/acs.jpclett.6c02173.pdf by VILNIUS UNIV user on 12 November 2026

relationship to biogenic sedimentation. *Global Biogeochem. Cy.* **1995**, *9*, 359−372.
(2) Field, C. B.; Behrenfeld, M. J.; Randerson, J. T.; Falkowski, P. Primary Production of the Biosphere: Integrating Terrestrial and Oceanic Components. *Science* **1998**, *281*, 237−240.
(3) Falkowski, P. G.; Barber, R. T.; Smetacek, V. Biogeochemical Controls and Feedbacks on Ocean Primary Production. *Science* **1998**, *281*, 200−206.
(4) Wagner, H.; Jakob, T.; Wilhelm, C. Balancing the energy flow from captured light to biomass under fluctuating light conditions. *New Phytol* **2006**, *169*, 95−108.
(5) Falciatore, A.; Jaubert, M.; Bouly, J.-P.; Bailleul, B.; Mock, T. Diatom Molecular Research Comes of Age: Model Species for Studying Phytoplankton Biology and Diversity. *Plant Cell* **2020**, *32*, 547−572.
(6) Büchel, C. Fucoxanthin-Chlorophyll Proteins in Diatoms: 18 and 19 kDa Subunits Assemble into Different Oligomeric States. *Biochemistry* **2003**, *42*, 13027−13034.
(7) Wang, W.; Yu, L.-J.; Xu, C.; Tomizaki, T.; Zhao, S.; Umena, Y.; Chen, X.; Qin, X.; Xin, Y.; Suga, M.; et al. Structural basis for blue-green light harvesting and energy dissipation in diatoms. *Science* **2019**, *363*, No. eaav0365.
(8) Pi, X.; Zhao, S.; Wang, W.; Liu, D.; Xu, C.; Han, G.; Kuang, T.; Sui, S.-F.; Shen, J.-R. The pigment-protein network of a diatom photosystem II−light-harvesting antenna supercomplex. *Science* **2019**, *365*, No. eaax4406.
(9) Nagao, R.; Kato, K.; Suzuki, T.; Ifuku, K.; Uchiyama, I.; Kashino, Y.; Dohmae, N.; Akimoto, S.; Shen, J.-R.; Miyazaki, N.; et al. Structural basis for energy harvesting and dissipation in a diatom PSII−FCPII supercomplex. *Nat. Plants* **2019**, *5*, 890−901.
(10) Nagao, R.; Kato, K.; Ifuku, K.; Suzuki, T.; Kumazawa, M.; Uchiyama, I.; Kashino, Y.; Dohmae, N.; Akimoto, S.; Shen, J.-R.; et al. Structural basis for assembly and function of a diatom photosystem I-light-harvesting supercomplex. *Nat. Commun.* **2020**, *11*, 2481.
(11) Xu, C.; Pi, X.; Huang, Y.; Han, G.; Chen, X.; Qin, X.; Huang, G.; Zhao, S.; Yang, Y.; Kuang, T.; et al. Structural basis for energy transfer in a huge diatom PSI-FCPI supercomplex. *Nat. Commun.* **2020**, *11*, 5081.
(12) Nagao, R.; Kato, K.; Kumazawa, M.; Ifuku, K.; Yokono, M.; Suzuki, T.; Dohmae, N.; Akita, F.; Akimoto, S.; Miyazaki, N.; et al. Structural basis for different types of hetero-tetrameric light-harvesting complexes in a diatom PSII-FCPII supercomplex. *Nat. Commun.* **2022**, *13*, 1764.
(13) Feng, Y.; Li, Z.; Yang, Y.; Shen, L.; Li, X.; Liu, X.; Zhang, X.; Zhang, J.; Ren, F.; Wang, Y.; et al. Structures of PSI-FCPI from *Thalassiosira pseudonana* grown under high light provide evidence for convergent evolution and light-adaptive strategies in diatom FCPIs. *J. Integr. Plant Biol.* **2025**, *67*, 949−966.
(14) Zhao, S.; Shen, L.; Li, X.; Tao, Q.; Li, Z.; Xu, C.; Zhou, C.; Yang, Y.; Sang, M.; Han, G.; et al. Structural insights into photosystem II supercomplex and trimeric FCP antennae of a centric diatom *Cyclotella meneghiniana*. *Nat. Commun.* **2023**, *14*, 8164.
(15) Papagiannakis, E.; van Stokkum, I. H. M.; Fey, H.; Büchel, C.; van Grondelle, R. Spectroscopic Characterization of the Excitation Energy Transfer in the Fucoxanthin−Chlorophyll Protein of Diatoms. *Photosynth. Res.* **2005**, *86*, 241−50.
(16) Gildenhoff, N.; Amarie, S.; Gundermann, K.; Beer, A.; Büchel, C.; Wachtveitl, J. Oligomerization and Pigmentation Dependent Excitation Energy Transfer in Fucoxanthin-Chlorophyll Proteins. *Biochim. Biophys. Acta - Bioenerg.* **2010**, *1797*, 543−549.
(17) Songaila, E.; Augulis, R.; Gelzinis, A.; Butkus, V.; Gall, A.; Büchel, C.; Robert, B.; Zigmantas, D.; Abramavicius, D.; Valkunas, L. Ultrafast energy transfer from chlorophyll c_2 to chlorophyll *a* in fucoxanthin−chlorophyll protein complex. *J. Phys. Chem. Lett.* **2013**, *4*, 3590−3595.
(18) Nagao, R.; Yokono, M.; Tomo, T.; Akimoto, S. Control Mechanism of Excitation Energy Transfer in a Complex Consisting of Photosystem II and Fucoxanthin Chlorophyll a/c-Binding Protein. *J. Phys. Chem. Lett.* **2014**, *5*, 2983−2987.
(19) Ramanan, C.; Berera, R.; Gundermann, K.; van Stokkum, I.; Büchel, C.; van Grondelle, R. Exploring the mechanism(s) of energy dissipation in the light harvesting complex of the photosynthetic algae *Cyclotella meneghiniana*. *Biochim. Biophys. Acta - Bioenerg.* **2014**, *1837*, 1507−1513.
(20) Gelzinis, A.; Butkus, V.; Songaila, E.; Augulis, R.; Gall, A.; Büchel, C.; Robert, B.; Abramavicius, D.; Zigmantas, D.; Valkunas, L. Mapping energy transfer channels in fucoxanthin−chlorophyll protein complex. *Biochim. Biophys. Acta - Bioenerg.* **2015**, *1847*, 241−247.
(21) Butkus, V.; Gelzinis, A.; Augulis, R.; Gall, A.; Büchel, C.; Robert, B.; Zigmantas, D.; Valkunas, L.; Abramavicius, D. Coherence and population dynamics of chlorophyll excitations in FCP complex: Two-dimensional spectroscopy study. *J. Chem. Phys.* **2015**, *142*, 212414.
(22) West, R. G.; Bína, D.; Fuciman, M.; Kuznetsova, V.; Litvín, R.; Polívka, T. Ultrafast multi-pulse transient absorption spectroscopy of fucoxanthin chlorophyll *a* protein from *Phaeodactylum tricornutum*. *Biochim. Biophys. Acta - Bioenerg.* **2018**, *1859*, 357−365.
(23) Elnour, H. M.; Dietzel, L.; Ramanan, C.; Büchel, C.; van Grondelle, R.; Krüger, T. P. Energy dissipation mechanisms in the FCPb light-harvesting complex of the diatom *Cyclotella meneghiniana*. *Biochim. Biophys. Acta - Bioenerg.* **2018**, *1859*, 1151−1160.
(24) Nagao, R.; Yokono, M.; Ueno, Y.; Shen, J.-R.; Akimoto, S. Low-Energy Chlorophylls in Fucoxanthin Chlorophyll a/c-Binding Protein Conduct Excitation Energy Transfer to Photosystem I in Diatoms. *J. Phys. Chem. B* **2019**, *123*, 66−70.
(25) Akhtar, P.; Feng, Y.; Jana, S.; Wang, W.; Shen, J.-R.; Tan, H.-S.; Lambrev, P. H. Ultrafast Energy Transfer in a Diatom Photosystem II Supercomplex. *J. Phys. Chem. Lett.* **2024**, *15*, 5838−5847.
(26) Gelzinis, A.; Chmeliov, J.; Tutkus, M.; Vitulskienė, E.; Franckevičius, M.; Büchel, C.; Robert, B.; Valkunas, L. Fluorescence quenching in aggregates of fucoxanthin-chlorophyll protein complexes: Interplay of fluorescing and dark states. *Biochim. Biophys. Acta - Bioenerg.* **2024**, *1865*, 149030.
(27) Akhtar, P.; Feng, Y.; Wang, W.; Shen, J.-R.; Büchel, C.; Tan, H.-S.; Lambrev, P. H. Excitonic network organization enables efficient energy transfer in diatom photosystem I. *Cell Rep. Phys. Sci.* **2025**, *6*, 102731.
(28) Ueno, Y.; Li, O.-Y.; Shen, J.-R.; Tomo, T.; Akimoto, S.; Nagao, R. Aggregation-Induced Excitation-Energy Quenching in Fucoxanthin Chlorophyll a/c-Binding Proteins from the Diatom *Phaeodactylum tricornutum*. *J. Phys. Chem. B* **2025**, *129*, 3553−3558.
(29) Miloslavina, Y.; Grouneva, I.; Lambrev, P. H.; Lepetit, B.; Goss, R.; Wilhelm, C.; Holzwarth, A. R. Ultrafast fluorescence study on the location and mechanism of non-photochemical quenching in diatoms. *Biochim. Biophys. Acta - Bioenerg.* **2009**, *1787*, 1189−1197.
(30) Chukhutsina, V. U.; Büchel, C.; van Amerongen, H. Variations in the first steps of photosynthesis for the diatom *Cyclotella meneghiniana* grown under different light conditions. *Biochim. Biophys. Acta - Bioenerg.* **2013**, *1827*, 10−18.
(31) Chukhutsina, V. U.; Büchel, C.; van Amerongen, H. Disentangling two non-photochemical quenching processes in *Cyclotella meneghiniana* by spectrally-resolved picosecond fluorescence at 77K. *Biochim. Biophys. Acta - Bioenerg.* **2014**, *1837*, 899−907.
(32) Oka, K.; Ueno, Y.; Yokono, M.; Shen, J.-R.; Nagao, R.; Akimoto, S. Adaptation of light-harvesting and energy-transfer processes of a diatom *Phaeodactylum tricornutum* to different light qualities. *Photosynth. Res.* **2020**, *146*, 227−234.
(33) Akimoto, S.; Ueno, Y.; Yokono, M.; Shen, J.-R.; Nagao, R. Adaptation of light-harvesting and energy-transfer processes of a diatom *Chaetoceros gracilis* to different light qualities. *Photosynth. Res.* **2020**, *146*, 87−93.
(34) Lee, S. E.; van de Poll, W.; Chukhutsina, V. Antarctic photosynthesis: energy transfer and charge separation in the diatom *Chaetoceros simplex*. *Biochim. Biophys. Acta - Bioenerg.* **2025**, *1866*, 149560.
(35) Gobets, B.; van Stokkum, I. H. M.; Rögner, M.; Kruip, J.; Schlodder, E.; Karapetyan, N. V.; Dekker, J. P.; van Grondelle, R. Time-Resolved Fluorescence Emission Measurements of Photosystem

Downloaded from pubs.acs.org/jpclcd/article-pdf/17/35/10191/6688584/acs.jpclett.6c02173.pdf by VILNIUS UNIV user on 12 November 2026

https://doi.org/10.1021/acs.jpclett.6c02173
J. Phys. Chem. Lett. 2026, 17, 10191−10198

I Particles of Various Cyanobacteria: A Unified Compartment Model. *Biophys. J.* **2001**, *81*, 407−424.
(36) Chmeliov, J.; Gelzinis, A.; Songaila, E.; Augulis, R.; Duffy, C. D. P.; Ruban, A. V.; Valkunas, L. The nature of self-regulation in photosynthetic light-harvesting antenna. *Nat. Plants* **2016**, *2*, 16045.
(37) Chmeliov, J.; Gelzinis, A.; Franckevičius, M.; Tutkus, M.; Saccon, F.; Ruban, A. V.; Valkunas, L. Aggregation-Related Non-photochemical Quenching in the Photosynthetic Membrane. *J. Phys. Chem. Lett.* **2019**, *10*, 7340−7346.
(38) Golubewa, L.; Padrez, Y.; Zemaityte, P.; Rutkauskas, D.; Büchel, C.; Gelzinis, A. Whole-cell glycerol-free fluorescence cryo-spectroscopy reveals electronic excitation dynamics in the diatom *Cyclotella meneghiniana*. *JACS Au* **2026**, DOI: 10.1021/jacsau.6c00630.
(39) van Stokkum, I. H.; Larsen, D. S.; van Grondelle, R. Global and target analysis of time-resolved spectra. *Biochim. Biophys. Acta - Bioenerg.* **2004**, *1657*, 82−104.
(40) Andrizhiyevskaya, E. G.; Chojnicka, A.; Bautista, J. A.; Diner, B. A.; van Grondelle, R.; Dekker, J. P. Origin of the F685 and F695 fluorescence in Photosystem II. *Photosynth. Res.* **2005**, *84*, 173−180.
(41) Kuczynska, P.; Jemiola-Rzeminska, M.; Strzalka, K. Photosynthetic Pigments in Diatoms. *Mar. Drugs* **2015**, *13*, 5847−5881.
(42) Groot, M.-L.; Frese, R. N.; de Weerd, F. L.; Bromek, K.; Pettersson, Å.; Peterman, E. J.; van Stokkum, I. H.; van Grondelle, R.; Dekker, J. P. Spectroscopic Properties of the CP43 Core Antenna Protein of Photosystem II. *Biophys. J.* **1999**, *77*, 3328−3340.
(43) Groot, M. L.; Peterman, E. J.; van Kan, P. J.; van Stokkum, I. H.; Dekker, J. P.; van Grondelle, R. Temperature-dependent triplet and fluorescence quantum yields of the photosystem II reaction center described in a thermodynamic model. *Biophys. J.* **1994**, *67*, 318−330.
(44) Groot, M.; Peterman, E.; van Stokkum, I.; Dekker, J.; van Grondelle, R. Triplet and fluorescing states of the CP47 antenna complex of photosystem II studied as a function of temperature. *Biophys. J.* **1995**, *68*, 281−290.
(45) Acharya, K.; Neupane, B.; Reppert, M.; Feng, X.; Jankowiak, R. On the Unusual Temperature-Dependent Emission of the CP47 Antenna Protein Complex of Photosystem II. *J. Phys. Chem. Lett.* **2010**, *1*, 2310−2315.
(46) Juhas, M.; Büchel, C. Properties of photosystem I antenna protein complexes of the diatom *Cyclotella meneghiniana*. *J. Exp. Bot.* **2012**, *63*, 3673−3681.
(47) Garbers, A.; Reifarth, F.; Kurreck, J.; Renger, G.; Parak, F. Correlation between Protein Flexibility and Electron Transfer from $Q_A^{-\bullet}$ to Q_B in PSII Membrane Fragments from Spinach. *Biochemistry* **1998**, *37*, 11399−11404.
(48) Raszewski, G.; Renger, T. Light Harvesting in Photosystem II Core Complexes Is Limited by the Transfer to the Trap: Can the Core Complex Turn into a Photoprotective Mode? *J. Am. Chem. Soc.* **2008**, *130*, 4431−4446.
(49) Shibata, Y.; Nishi, S.; Kawakami, K.; Shen, J.-R.; Renger, T. Photosystem II Does Not Possess a Simple Excitation Energy Funnel: Time-Resolved Fluorescence Spectroscopy Meets Theory. *J. Am. Chem. Soc.* **2013**, *135*, 6903−6914.
(50) Beer, A.; Gundermann, K.; Beckmann, J.; Büchel, C. Subunit Composition and Pigmentation of Fucoxanthin-Chlorophyll Proteins in Diatoms: Evidence for a Subunit Involved in Diadinoxanthin and Diatoxanthin Binding. *Biochemistry* **2006**, *45*, 13046−13053.
(51) Nguyen, H. L.; Do, T. N.; Zhong, K.; Akhtar, P.; Jansen, T. L. C.; Knoester, J.; Caffarri, S.; Lambrev, P.; Tan, H.-S. Inter-subunit energy transfer processes in a minimal plant photosystem II supercomplex. *Sci. Adv.* **2024**, *10*, No. eadh0911.
(52) Provasoli, L.; McLaughlin, J.; Droop, M. The development of artificial media for marine algae. *Archiv. Mikrobiol* **1957**, *25*, 392−428.
(53) R Development Core Team. *R: A Language and Environment for Statistical Computing*; R Foundation for Statistical Computing: Vienna, Austria, 2015.

Downloaded from pubs.acs.org/jpclcd/article-pdf/17/35/10191/6688584/acs.jpclett.6c02173.pdf by VILNIUS UNIV user on 12 November 2026

https://doi.org/10.1021/acs.jpclett.6c02173
J. Phys. Chem. Lett. 2026, 17, 10191−10198